Comparison of 4 Methods for Quantification of Dopamine Transporters by SPECT with [^{123}I]IACFT

Ali A. Bonab, Alan J. Fischman, and Nathaniel M. Alpert

Division of Nuclear Medicine, Department of Radiology, Massachusetts General Hospital, Boston; and Department of Radiology, Harvard Medical School, Boston, Massachusetts

2β-Carbomethoxy-3β-(4-fluorophenyl)-n-(1-iodoprop-1-en-3-yl) nortropane (IACFT) is a highly selective ligand for dopamine transporter (DAT) sites in the striatum. Recent reports have described the basic kinetics, neurobiology, and imaging properties of [^{123}I]IACFT. This report focuses on the structural (i.e., the ability to produce consistent binding estimates) validity of 4 methods to quantify striatal binding potential (BP) for IACFT. **Methods:** Seven healthy volunteers and 8 patients with Parkinson's disease were subjects for this study. Dynamic SPECT images and arterial blood samples were acquired during the 1.5–2 h after injection of 185–370 MBq [^{123}I]IACFT. Plasma radioactivity was analyzed chromatographically to obtain metabolite-corrected arterial input functions. The k_3/k_4 ratio (BP) for striatal DAT sites was calculated by 4 methods. In the first method, tissue time–activity curves and metabolite-corrected arterial input functions were analyzed by a linear graphic method developed for reversible receptor ligands. The second method was also graphic; however, the occipital cortex time–activity curve was used as the input function. In the third method, the difference between the striatal and occipital cortex time–activity curves at secular equilibrium was taken to represent bound tracer, the occipital cortex time–activity curve was used to represent tracer in the free and nonspecifically bound state, and equilibrium receptor equations were used to determine BP. The fourth method used the occipital cortex time–activity curve to mathematically derive an input function for fitting the striatal time–activity curve and to determine BP. **Results:** Analysis of the dynamic SPECT data by methods 1 and 2 resulted in highly linear plots (after approximately 15 min), supporting the reversibility of the tracer. A high linear correlation was found for BP determined by all 4 methods. ANOVA showed that methods 1–3 were indistinguishable; method 4 yielded lower BPs than did methods 1–3. **Conclusion:** These results show that BP can be estimated consistently using 4 different methods. This finding lends support to the modeling assumptions and provides methods suitable for clinical investigation.

Key Words: dopamine transporter; kinetic modeling; SPECT quantification; Parkinson's disease; brain SPECT

J Nucl Med 2000; 41:1086–1092

The integrity of the presynaptic dopamine system can now be evaluated by several methods that involve radiolabeled compounds and external imaging. A remaining challenge is to establish ligands and methods suitable for clinical investigation of degenerative diseases. The dopa decarboxylase activity of nigrostriatal neurons can be measured with [^{18}F]6-fluorodopa and dynamic PET. However, this tracer is not ideal because its peripheral metabolites cross the blood–brain barrier and must be considered to achieve quantitative assay. An alternative approach is to measure the binding potential (BP) of dopamine transporter (DAT) sites. Ligands available for that purpose include [^{123}I]β-CIT, [^{11}C]β-CIT, [^{99m}Tc]TRODAT, [^{123}I]FPCIT, and [^{11}C]CFT. Although these tracers have been used successfully in a large number of research studies (*1–7*), their properties are not ideal for clinical applications. β-CIT ([^{123}I] β-2 βcarboxymethoxy-3β-(4-iodophenyl)tropane) has a high affinity for the DAT in the striatum; however, autoradiographic and SPECT studies have shown that, like cocaine, it concentrates in both dopamine- and 5-hydroxytryptamine (5-HT)–rich regions of the brain (*1,2*). Furthermore, a delay of 24 h between injection and imaging with β-CIT is required for quantitation of DAT sites in the human striatum (*1,2*), and radiolabeled lipophilic metabolites may complicate quantitation of DAT density (*6*). More recently, the ligand [^{11}C]CFT has been introduced, and although it has excellent imaging properties with PET, peripheral metabolism of the tracer should be measured in each patient and care taken to account for significant levels of nonspecific binding (*4*).

The ligands [^{99m}Tc]TRODAT ([^{99m}Tc][2-[[2[[[3-(4-chlorophenyl)-8-methyl-8-azablcyclo[3.2.1] oct-2y-yl] methyl] (2-mercaptoethyl)amino]-ethyl]-amino]ethane-thiolato(3-)-N2,N2′,S2,S2′]oxo-[1R-(exo-exo)]) and [^{123}I]FPCIT ([^{123}I] N-ω-fluoropropyl-2β-carbomethoxy-3β-(4-iodophenyl)nortropane) have excellent clinical imaging properties, but they dissociate slowly from the DAT (*7,8*), making quantification of their BP difficult.

Previous work by our group suggested that [^{123}I]2β-carbomethoxy fluorophenyl)-*N*-(-3β-(4-1-iodoprop-1-en-3-yl)nortropane (E-IACFT, designated as Altropane; Boston Life Sciences, Inc., Boston, MA) has desirable properties for clinical application (*9*). In particular, the ^{123}I label permits imaging with a widely available technique, SPECT (*10*). On the basis of in vitro binding studies with [^{3}H]CFT and [^{3}H]citalopram (a high-affinity and selective ligand for 5-HT

Received Apr. 8, 1999; revision accepted Sep. 23, 1999.

For correspondence or reprints contact: Nathaniel M. Alpert, PhD, Division of Nuclear Medicine, Department of Radiology, Massachusetts General Hospital, 32 Fruit St., Boston, MA 02114.

transporter sites (*3*), E-IACFT was shown to have high affinity (inhibitory concentration of 50% = 6.62 ± 0.78 nmol) and selectivity (dopamine–to–5-HT ratio = 25:1) for DAT sites. Autoradiographic and SPECT studies in monkeys showed rapid and extremely high levels of accumulation in the striatum and minimal activity in other brain regions (*9,11–14*). Important for quantitative assay of the DAT sites is the fact that E-IACFT dissociates rapidly from the receptor and thus can be considered a reversible tracer.

A key step in the validation of any in vivo receptor assay is the development and evaluation of appropriate kinetic analyses. In the current study, we show consistent binding data with 4 separate analyses in 7 healthy volunteers and 8 patients with Parkinson's disease. Data from these subjects and preliminary kinetic analyses have been reported previously (*15*). In this study, 4 different methods of kinetic analysis were compared in the same group of subjects. The procedures for data analysis included graphic methods requiring blood sampling and metabolite correction; a reference region graphic technique that does not require blood sampling or metabolite correction; a secular equilibrium method, similar to that originally used for analysis of studies with [^{11}C]raclopride (*16*); and a reference tissue fitting method (*17*).

MATERIALS AND METHODS

Human Subjects

Seven healthy volunteers (5 men [age range, 37–75 y], 2 women [aged 26 and 39 y]) and 8 patients with Parkinson's disease (age range, 14–79 y; Hoehn and Yahr stages 1.5–3 [n = 5] and 4 or 5 [n = 3]) participated in these studies. Additional details about the study population have been reported (*15*). To reduce thyroid uptake of ^{123}I, all subjects received 0.6 g saturated solution of potassium iodide daily for 7 d beginning 48 h before radiopharmaceutical injection.

The imaging protocol was approved by the committees on human studies, pharmacy, and radioisotopes of the Massachusetts General Hospital. All subjects gave written informed consent before participation in the study.

Preparation of [^{123}I]IACFT and Metabolite Analysis

[^{123}I]IACFT was prepared and metabolites in plasma were analyzed by reported methods (*15*). With these procedures, [^{123}I]IACFT was obtained in a radiochemical yield of approximately 65%, a radiochemical purity of greater than 98%, and a specific activity of approximately 185 GBq/μmole. To confirm that the product was free of pyrogens, the limulus test was performed before injection. Sterility was verified after injection. Plasma was analyzed by chromatography on C_{18} SepPaks (Waters, Milford, MA) that were activated with methanol and washed sequentially twice with phosphate buffer (pH, 7.4) and once with methanol.

SPECT

Images were acquired with a MultiSPECT 2 γ camera (Siemens Medical Systems, Inc., Hoffman Estates, IL) equipped with fan-beam collimators. The primary imaging parameters of this device are an intrinsic resolution of 4.6 mm (x and y directions) full width at half maximum and a sensitivity of approximately 236 Hz/μCi. Images were acquired over 360° (60 projections per head, 128 × 128 matrix) in the continuous imaging mode and were reconstructed using a conventional filtered backprojection algorithm to an in-plane resolution of 10 mm full width at half maximum. Attenuation correction was performed using the Chang algorithm (*18*). The SPECT camera was cross calibrated with a well scintillation counter by comparing the camera response from a uniform distribution of a ^{123}I solution in a 15-cm cylindric phantom with the response of the well counter to an aliquot of the same solution.

Before imaging, a venous catheter was placed in an antecubital vein for radiopharmaceutical administration and a radial arterial catheter was placed in the opposite wrist for blood sampling. The subjects were positioned supine on the imaging bed of the SPECT camera with arms extended outside the field of view and head immobilized with individually fabricated head holders (Tru-Scan Imaging, Annapolis MD). Approximately 370 MBq [^{123}I]IACFT were injected intravenously during 60 s, and serial SPECT images were acquired. Dynamic SPECT was started at the end of the infusion in 2-min acquisitions for the first hour and 5-min acquisitions for the second hour. Arterial blood samples (1 mL) were collected at 20-s intervals for the first 5 min, 1.0-min intervals for the next 15 min, and 5.0-min intervals thereafter. At 1, 5, 10, 30, 60, and 90 min, 5-mL blood samples were obtained for metabolite analysis.

Image Analysis

The SPECT slices with the highest striatal activity and those in which the occipital cortex was visualized were summed during a 90-min period to increase signal-to-noise ratio, and 5 regions of interest (ROIs) were defined. In the striatal planes, ROIs were placed on the right and left striatum, frontal cortex, and occipital pole. Concentrations from the right and left striatum were averaged. A single ROI was placed on the occipital cortex. Average ROI concentrations (cpm/mL) were decay corrected to the time of injection and expressed as kBq/mL using a calibration factor of

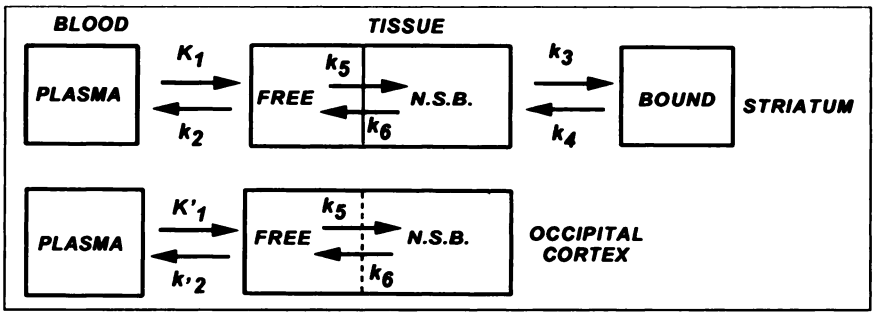

Figure 1. Compartmental models illustrating receptor kinetics of [^{123}I]IACFT in human brain. Three-compartment model (top) was used to analyze striatal time–activity data, and 2-compartment model (bottom) was used to fit occipital cortical data. N.S.B. = nonspecifically bound.

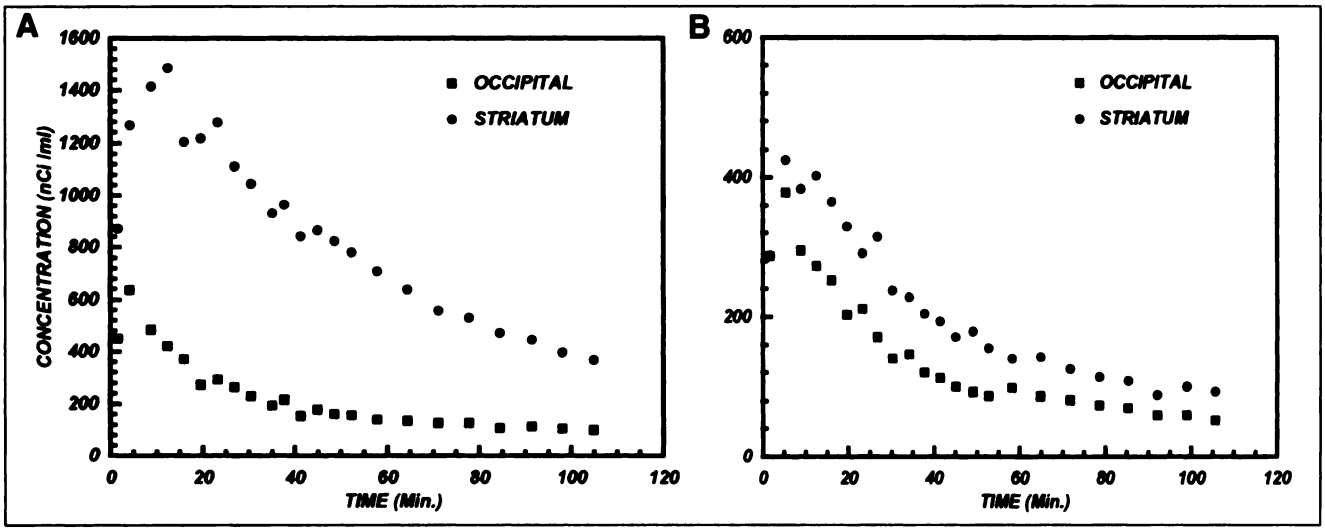

Figure 2. Representative time–activity curves for striatum and occipital cortex (expressed as nCi/mL) in healthy volunteer (A) and patient with severe Parkinson's disease (B).

0.12506 kBq/cpm. Corrections for partial-volume effects or scatter fraction were not performed.

Kinetic Modeling

Figure 1 illustrates the common kinetic model that underlies the different methods used to analyze the [^{123}I]IACFT SPECT data. All analyses assumed instantaneous equilibrium between free and nonspecifically bound ligand. In the discussion that follows, we use the term "free ligand" to refer to a ligand in either the free or the nonspecifically bound state. Conceptually, [^{123}I]IACFT can be in 1 of 3 states: free ligand in blood plasma, free ligand in tissue, or ligand associated with DAT sites. The rate constants K_1 (mL/min/g) and k_2 (per minute) provide a summary description of ligand transport into and out of the free compartment in tissue, and k_3 (i.e., $k_{on} \times B'_{max}$ [per minute]) and k_4 (k_{off} [per minute]) describe the bimolecular binding to, and dissociation from, DA transporters. For the occipital cortex, k_3 and k_4 were assumed to be zero, and this tissue was used as a reference to calculate the ratio K_1/k_2. The BP for [^{123}I]IACFT interaction with DAT sites was calculated to provide an index of specific binding as the ratio $BP = k_3/k_4 = k_2 \times B'_{max}/(K_D \times K_1)$.

Method 1. The time–activity data were analyzed by the linear graphic method developed by Logan et al. (*19*) for reversible receptor ligands. The integrated tissue activity from time zero to T was corrected for intravascular tracer with a fixed fractional volume (V_p), normalized to tissue activity at time T, and plotted against the metabolite-corrected integrated plasma time–activity data, which were also normalized to tissue activity at time T. This "Logan plot" becomes linear when pseudoequilibrium is reached, and assuming that nonspecific binding is negligible, the asymptotic slope for striatal data equals $K_1/k_2[1 + k_3/k_4]$. In contrast, because one can assume that DA transporters are not present in occipital cortex, k_3 and k_4 are negligible and the asymptotic slope equals K_1/k_2. Thus, assuming the ratio K_1/k_2 is the same for striatum and occipital cortex, the measured ratio of slopes depends on only k_3/k_4. Linear least squares regression was used to estimate the slope from the linear portion of the graphs.

Method 2. Method 2 was similar to the first, except that a reference region time–activity curve was used as the input to calculate distribution volume ratio (DVR) for the striatum. The DVR approach (*18,19*) is an attractive method for analysis of the kinetics of reversible ligands without blood sampling. For calculating DVR, the integrated tissue radioactivity from time zero to T, normalized to tissue activity at time T, was plotted versus the integrated occipital time–activity data, which were also normalized to tissue activity at time T (Eq. 1). This plot becomes linear when

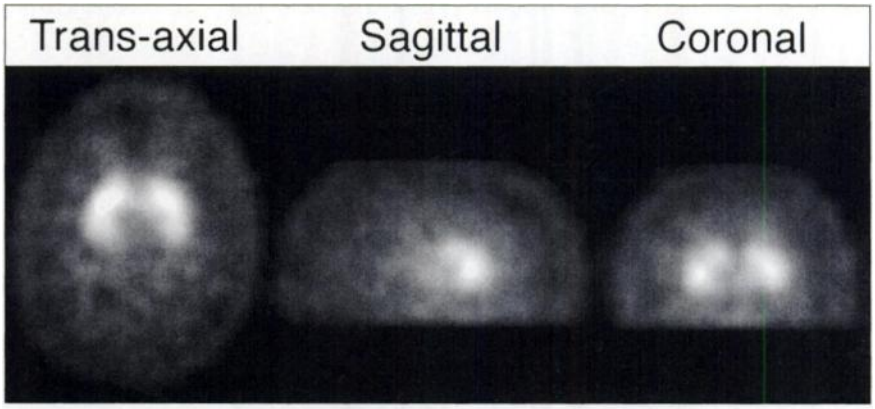

Figure 3. Transaxial, sagittal, and coronal SPECT images of brain of healthy volunteer 30–45 min after injection of 370 MBq [^{123}I]IACFT.

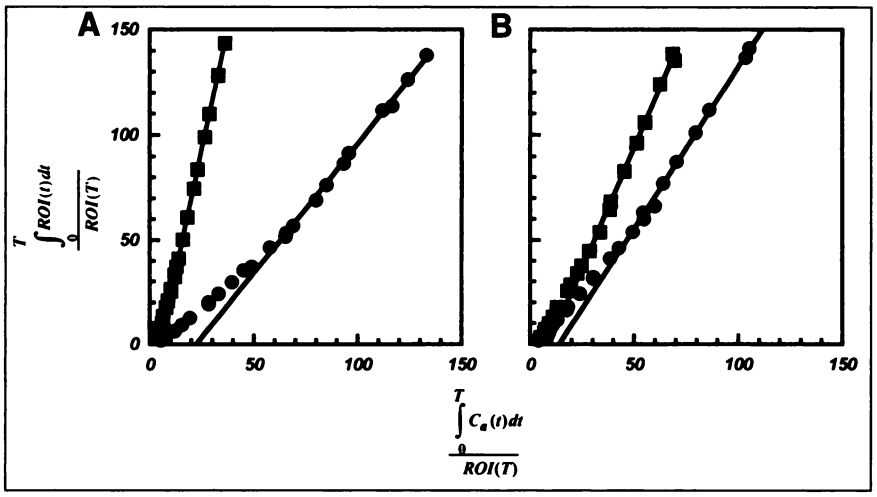

Figure 4. Representative "Logan plots" for striatum (■) and occipital cortex (●) derived from SPECT data from healthy volunteer (A) and patient with severe Parkinson's disease (B).

pseudoequilibrium is reached and the asymptotic slope for striatal data equals DVR; BP = DVR − 1.

$$\frac{\int_0^T A(t)\,dt}{A(T)} = DVR\frac{\int_0^T Occ(t)\,dt}{A(T)} + C_1\frac{Occ(T)}{A(T)} + C_2. \quad \text{Eq. 1}$$

DVR was estimated using multiple regression analysis (*20,21*).

Method 3. Method 3 was an adaptation of 1 of the procedures that has been used to quantify [^{11}C]raclopride binding to dopamine D_2 receptors (*16*). Briefly, the key assumption of this method is that at secular equilibrium the classic equilibrium kinetic model of bimolecular binding can be applied. With the assumption that nonspecific binding is negligible in the striatum and occipital cortex, the striatal time–activity curve (Str_{TAC}) represents the kinetic behavior of specifically bound ligand plus free ligand, whereas the occipital cortex time–activity curve (Occ_{TAC}) represents the kinetic behavior of free ligand. Under these assumptions, the function ($Str_{TAC} - Occ_{TAC}$) defines the time dependence of bound tracer. Fitting of this curve to a γ variate function ($At^n e^{-m\cdot t}$) and division of the maximum bound tracer concentration by the value of Occ_{TAC} at the same time yields the equilibrium estimate of k_3/k_4.

Method 4. Method 4 used the reference tissue model (*17*). In this model, the Occ_{TAC} is the input for fitting striatal time–activity curves. The reference tissue model assumes, first, that a reference tissue region devoid of specific binding exists; second, that nonspecific binding is the same in the reference and specific compartments; third, that labeled metabolites of the parent tracer do not cross the blood–brain barrier; and fourth, that nonspecific and free label exchange instantaneously so that they can be treated as a single compartment. When these 4 assumptions are satisfied the following equation can be derived:

$$C_T(t) = R_1C_R(t) + \left\{k_2 - \frac{R_1k_2}{1 + BP}\right\} C_R(t) \otimes e^{-[k_2/(1+BP)+\lambda]t}, \quad \text{Eq. 2}$$

where $C_R(t)$ is the concentration time course in the reference tissue, $C_T(t)$ is the concentration time course in the target tissue, R_1 is the ratio of ligand delivery to the target and reference tissues, k_2 is the efflux rate constant from the target tissue, λ is the physical decay constant of the isotope, and $\otimes$ is the convolution operator.

RESULTS

Figure 2 shows representative time–activity curves for the striatum and occipital cortex of a healthy volunteer and a patient with severe Parkinson's disease. These data show rapid cerebral uptake and egress of IACFT. After intravenous injection, accumulation of tracer in the striatum is rapid, reaches a maximum at 10–15 min after injection, and decreases, consistent with reversible binding, to near background levels by 2 h. In accord with the known low density of dopaminergic neurons in the occipital cortex, uptake is lower, it peaks earlier (5–10 min), and it decreases much more rapidly than does the striatal curve. Figure 3 shows images of high count density (summation of data acquired from 30 to 45 min after injection) displayed in transaxial, sagittal, and coronal projections. These data clearly indicate a high concentration of radiopharmaceutical in the striatum with minimal accumulation in other areas of the brain. In particular, lack of accumulation in the thalamus, hypothalamus, or midbrain—regions that are rich in 5-HT transporters—supports the specificity of this tracer for DAT sites (*12–14*).

Kinetic analysis by method 1, the "Logan plot," is illustrated in Figure 4 for both a healthy volunteer and a

TABLE 1
[^{123}I]Altropane Binding Potential Determined by 4 Methods of Analysis

Subject no.	Method 1	Method 2	Method 3	Method 4
1	1.25	1.33	1.54	1.95
2	1.51	1.51	1.86	1.87
3	1.37	1.50	1.49	1.77
4	1.81	1.95	1.89	2.38
5	1.57	1.79	1.93	2.24
6	2.81	3.01	2.67	3.38
7	0.71	0.72	0.65	0.85
8	0.53	0.50	0.61	0.78
9	0.54	0.51	0.46	0.64
10	0.49	0.58	0.66	0.81
11	0.61	0.55	0.49	0.50
12	1.02	0.95	1.06	1.08
13	1.01	0.98	0.89	1.24
14	1.00	0.99	0.80	1.24
15	0.69	0.69	0.69	0.77

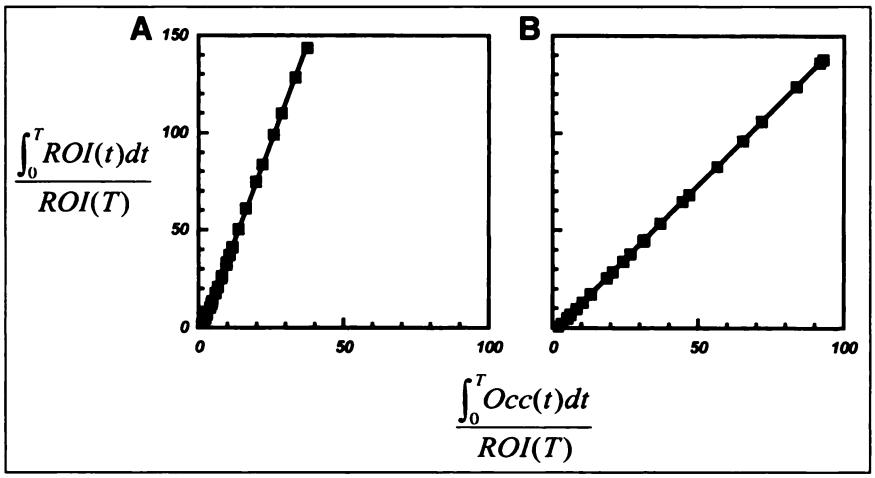

Figure 5. Representative reference region graphic plots for striatum using occipital cortex as reference in healthy volunteer (A) and patient with severe Parkinson's disease (B). Occ = occipital cortex.

patient with severe Parkinson's disease. In Figures 4A and B, the curves become linear soon after injection; however, the ratio of slopes is significantly reduced in the patient with Parkinson's disease. For occipital cortex and striatum, the slopes were interpreted in terms of 1- and 2-compartment models, respectively. In all subjects, the plots were linear for both tissues by approximately 30 min after injection. Thus, asymptotic slopes were calculated from the data acquired between 30 and 120 min after injection. In all subjects, the slope was greater for the striatum than for the occipital cortex. Because fitting of the occipital cortex time–activity curve to a 2-compartment model indicated that k_5/k_6 was negligible, the slope of the plot was K_1/k_2. Thus, the slope ratio yielded a value of BP + 1. The BP values determined by this method are given in Table 1.

Figures 5A and B illustrate the use of the reference region graphic plot, or method 2, in a healthy volunteer and a patient with severe Parkinson's disease. The graphs for striatal data using the occipital cortex as the reference become linear but had a lower DVR in the patient than in the volunteer. In all subjects, the plots were linear by approximately 30 min after injection. The DVRs were calculated from the data acquired 30–120 min after injection using a linear least squares fit to Equation 1. BP was taken to be DVR − 1, and the values of BP from this method are given in Table 1.

A key feature of analysis by method 3 is illustrated in Figure 6. Shown is a plot of (Str_{TAC} − Occ_{TAC}) and the corresponding γ-variate fit for a healthy volunteer and a patient with severe Parkinson's disease. The fitted curves are assumed to represent bound tracer, and at its maximum the tracer is in secular equilibrium. At the maximum, the ratio of bound (Str_{TAC} − Occ_{TAC}) to free (occipital cortex) tracer equals k_3/k_4, the BP. Accordingly, BPs were determined from the maxima of the fitted curves for each subject and are summarized in Table 1.

Figure 7 represents the fit to the striatal time–activity curve using the occipital time–activity curve as the reference tissue for method 4 in a healthy volunteer and a patient with severe Parkinson's disease. With this method, Equation 2 was fitted to 3 parameters—the ratio of ligand delivery to the target and reference tissue [$k_2 - R_1k_2/(1 + BP)$], and [$k_2/(1 + BP) + \lambda$]—and the BP was calculated using the values of these parameters (Table 1).

The data in Table 1 were analyzed using ANOVA to test the hypothesis that all 4 methods yield the same results. The statistical model used method (1, 2, 3, or 4) as a categoric variable, and hypotheses were tested by planned comparisons. The hypothesis that the 4 methods yielded the same results was rejected ($t = 64$, df = 56; $P < 0.001$). Further testing showed that methods 1–3 were equivalent ($t = 0.02$). Figure 8 shows correlations of the BP for the 4 methods used

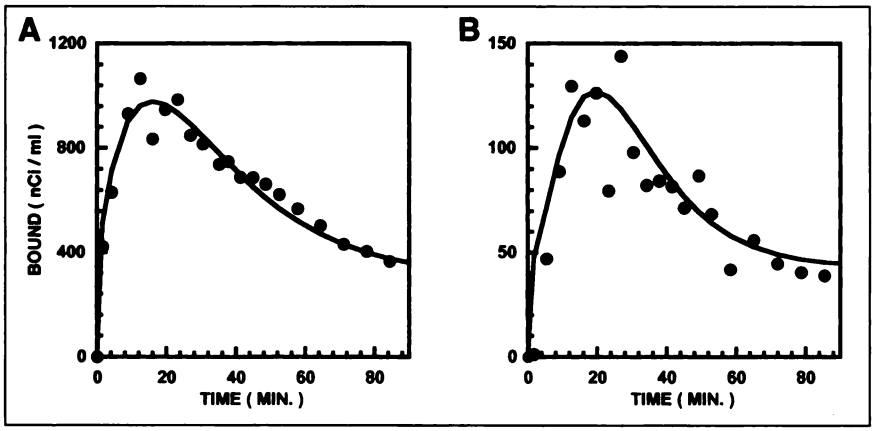

Figure 6. Plot of (Str_{TAC} − Occ_{TAC}) and corresponding γ variate fit for healthy volunteer (A) and patient with severe Parkinson's disease (B).

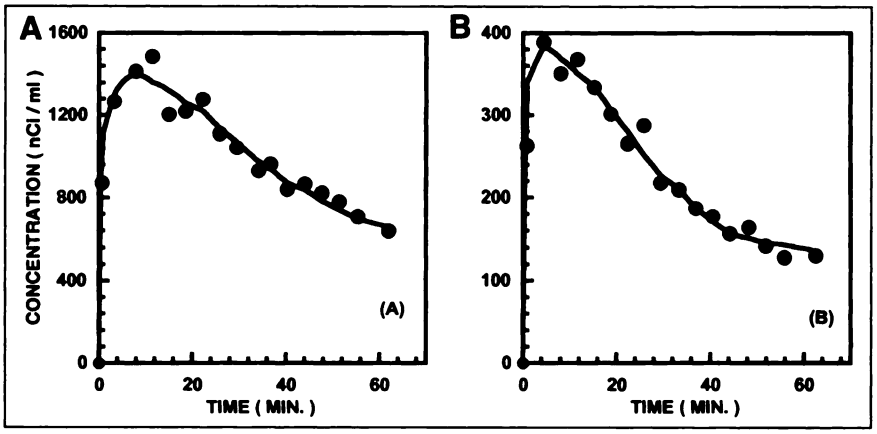

Figure 7. Representative fits of striatal time–activity curves using occipital time–activity curves as reference for reference tissue fitting method in healthy volunteer (A) and patient with severe Parkinson's disease (B).

to analyze [^{123}I]IACFT data. Consistent with the statistical analysis, the comparison-of-methods data are well represented by linear regressions. For methods 1–3, the slopes are all close to 1 and are not significantly different from one another. The slopes for method 4 versus the others are significantly higher.

DISCUSSION

The point of this paper was the structural validity of the analyses as assessed by analyzing the same data with different methods. BP was chosen as the endpoint for comparison. No corrections were made for protein binding, partial-volume, or finite resolution effects, and the resulting systematic errors were assumed to have a similar effect on BP in all 4 methods. Methods 1–3 provided similar values for BP, as is seen in Figure 8. Quantitative similarity of the first 3 methods was established by ANOVA. Method 4, although shown to differ quantitatively from the other methods by ANOVA, nevertheless was linearly related to the other methods ($R^2 > 0.95$). The fact that methods 1–3 yielded similar results is important because methods 2 and 3 did not require arterial cannulation. Compared with the other

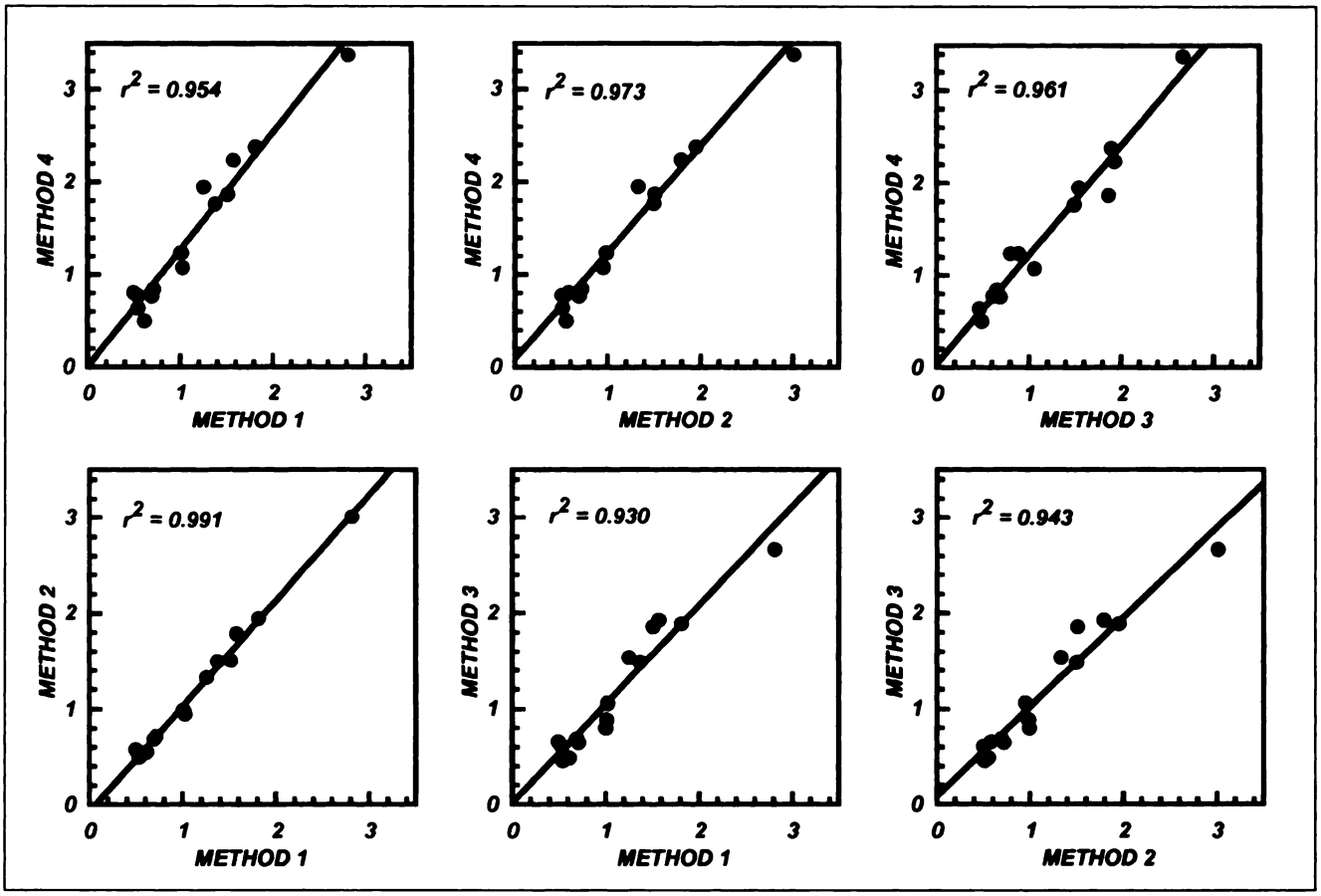

Figure 8. Linear regression of BP values for [^{123}I]IACFT determined by 4 methods used for data analysis.

methods, method 2 used a completely different approach to modeling the kinetics of IACFT. Method 4 appeared to yield quantitative values different from those of the other methods because it empirically determines the ratio of distribution volumes for striatum and occipital cortex, which, in these studies, differed from unity.

Our previous work established the biologic fate, selectivity, and binding characteristics of [^{123}I]IACFT (*12–14*). Initial results of in vivo binding assays have also been reported (*15*). In establishing the validity of a new in vivo ligand for PET or SPECT, the most definitive approach is direct measurement of the receptor binding characteristics, B'_{max} and K_D. This approach requires multiple measurements in the same experimental subject under conditions in which receptor occupancy is perturbed (*4*). In this study, we have addressed what might be called the structural validity of the in vivo assay by determining BP from the same dataset by several methods. Structural validity is supported by concordant estimates of BP by the different methods.

Figure 8 shows a strong linear relationship among all the methods, with $R^2 > 0.95$ in all instances. When these data were subjected to an ANOVA in which method was the categoric variable, we found that method 4 differed from the others but that methods 1–3 were indistinguishable. All 4 methods make 4 common assumptions—that the tracer is present in 3 forms (free ligand, nonspecifically bound, and specifically bound), that an instantaneous equilibrium exists at all times between free ligand and nonspecifically bound ligand, and that the interpretation of the data rests on use of the compartment model illustrated in Figure 1.

The two graphic methods, methods 1 and 2, yield equivalent assays despite the fact that method 1 requires a metabolite-corrected plasma input function whereas method 2 uses data from a reference region. Because the close agreement relies on the high selectivity of IACFT to provide a valid reference region devoid of dopaminergic neurons, this equivalency is important and supports the structural assumptions implicit in the modeling. Method 3 uses a completely different approach to the assay, focusing on the moment when a reversible tracer can be considered to be in secular equilibrium. Method 3 also relies on a reference region to estimate the free tracer plus nonspecifically bound tracer.

The close correspondence of methods 1–3 is striking and makes the systematic difference in the results of method 4 more interesting. Method 4 relies on nonlinear least squares fitting in which the reference region curve is used in place of a measured plasma curve. The key point is that methods 1–3 assume that K_1/k_2 is the same for the striatum and for the reference region, but method 4 does not assume that delivery of tracer to the striatum is the same as to the reference region.

CONCLUSION

Overall, the data strongly support the structural validity of BP measurements with [^{123}I]IACFT. The discrepancy between method 4 and the others is mitigated by the excellent linear correlation among the methods. On the basis of these findings, the choice of method may be based on convenience for the experiment at hand, and excellent results can be obtained without blood sampling.

ACKNOWLEDGMENTS

This study was supported in part by grants NS30556, DA06303, and T32-CA09362 from the National Institutes of Health, Bethesda, MD.

REFERENCES

1. Laruelle M, Baldwin RM, Malison RT, et al. SPECT imaging of dopamine and serotonin transporters with [^{123}I]beta-CIT: pharmacological characterization of brain uptake in nonhuman primates. *Synapse.* 1993;13:295–309.
2. Laruelle M, Wallace E, Seibyl JP, et al. Graphical, kinetic, and equilibrium analyses of in vivo [^{123}I]beta-CIT binding to dopamine transporters in healthy human subjects. *J Cereb Blood Flow Metab.* 1994;14:982–994.
3. D'Amato RJ, Largent BL, Snowman AM, Snyder SH. Selective labeling of serotonin uptake sites in rat brain by [^{3}H]citalopram contrasted to labeling of multiple sites by [^{3}H]imipramine. *J Pharmacol Exp Ther.* 1987;242:364–371.
4. Morris ED, Babich JW, Alpert NM, et al. Quantification of dopamine transporter density in monkeys by dynamic PET imaging of multiple injection of ^{11}C-CFT. *Synapse.* 1996;24:262–272.
5. Innis R, Baldwin R, Sybirska E, et al. Single photon emission computed tomography imaging of monoamine reuptake sites in primate brain with [^{123}I]CIT. *Eur J Pharmacol.* 1991;200:369–370.
6. Kushner, SA, McElgin WT, Kung, M, Mozley PD, et al. Kinetic modeling of [^{99m}Tc]TRODAT-1: dopamine transporter imaging agent. *J Nucl Med.* 1999;40:150–158.
7. Booij J, Hemelaar JT, Speelman D, de Bruin K, Janssen AG, van Royen EA. One-day protocol for imaging of nigrostriatal dopaminergic pathway in Parkinson's disease by [^{123}I]FPCIT SPECT. *J Nucl Med.* 1999;40:735–761.
8. Bergstrom KA, Halldin C, Kuikka JT, et al. Lipophilic metabolite of [^{123}I]beta-CIT in human plasma may obstruct quantitation of the dopamine transporter. *Synapse.* 1995;19:297–300.
9. Elmaleh DR, Fischman AJ, Shoup TM, et al. Preparation and biological evaluation of iodine-125-IACFT: a selective SPECT agent for imaging dopamine transporter sites. *J Nucl Med.* 1996;37:1197–1202.
10. Bonab AA, Babich JW, Alpert NM, Madras BK, Fischman AJ. Comparison of 3 methods for quantification of dopamine transporters by SPECT with I-123 altropane [abstract]. *J Nucl Med.* 1997;5(suppl):223P.
11. Fischman AJ, Babich JW, Elmaleh DR, et al. SPECT imaging of dopamine transporter sites in normal and MPTP treated rhesus monkeys. *J Nucl Med.* 1996;37:1197–1202.
12. Madras BK, Gracz LM, Meltzer PC, et al. Altropane, a SPECT or PET imaging probe for dopamine neurons: I. Dopamine transporter binding in primate brain. *Synapse.* 1998;29:93–104.
13. Madras BK, Gracz LM, Meltzer PC, et al. Altropane, a SPECT or PET imaging probe for dopamine neurons: II. Distribution to dopamine-rich regions of primate brain. *Synapse.* 1998;29:105–115.
14. Madras BK, Gracz LM, Kaufman MJ, et al. Altropane, a SPECT or PET imaging probe for dopamine neurons: III. Human dopamine transporter in postmortem normal and Parkinson's disease brain. *Synapse.* 1998;29:116–127.
15. Fischman AJ, Bonab AA, Babich JW, et al. Rapid detection of Parkinson's disease by SPECT with altropane: a selective ligand for dopamine transporters. *Synapse.* 1998;29:128–141.
16. Farde L, Eriksson L, Blomquist G, Halldin C. Kinetic analysis of central [^{11}C]raclopride binding to D_2-dopamine receptors studied by PET: a comparison to the equilibrium analysis. *J Cereb Blood Flow Metab.* 1989;9:696–708.
17. Gunn RN, Lammertsma AA, Cunningham VJ. Parametric imaging of ligand-receptor interaction using a reference tissue model. *Neuroimage.* 1997;6:279–287.
18. Chang L. A method for attenuation correction in computed tomography. *IEEE Trans Nucl Sci.* 1987;25:638–643.
19. Logan J, Fowler JS, Volkow ND, et al. Graphical analysis of reversible radioligand binding from time activity measurements applied to N-^{11}C-methyl-(−)-cocaine PET studies. *J Cereb Blood Flow Metab.* 1990;10:740–747.
20. Ichise M, Ballinger JR, Golan H, et al. Noninvasive quantification of D2 receptors with iodine-123-IBF SPECT. *J Nucl Med.* 1996;37:513–520.
21. Logan J, Fowler J, Volkow ND, Wang G, Ding Y, Alexoff DL. Distribution volume ratio without blood sampling from graphical analysis of PET data. *J Cereb Blood Flow Metab.* 1996;16:834–840.